where

$$Q_i = \left\{ \frac{4C_i C}{(\beta_i - \beta)^2} + 1 \right\}^{-1/2} \quad (4)$$

while

$$C_i = \frac{\sqrt{(2\Delta)}}{\rho} \frac{U_i^2}{V_i^3} \frac{K_0(W_i d/\rho)}{K_1^2(W_i)} \quad (5)$$

and U_i, V_i, W_i are the standard waveguide parameters of the i-polarised mode of fibre 1.[4] C is obtained by replacing U_i, V_i, W_i with U, V, W in eqn. 5, where U, V, W are the waveguide parameters for fibre 2. Δ is the usual index height, which may be different for different polarisations and/or fibres, but we neglect such a small variation.

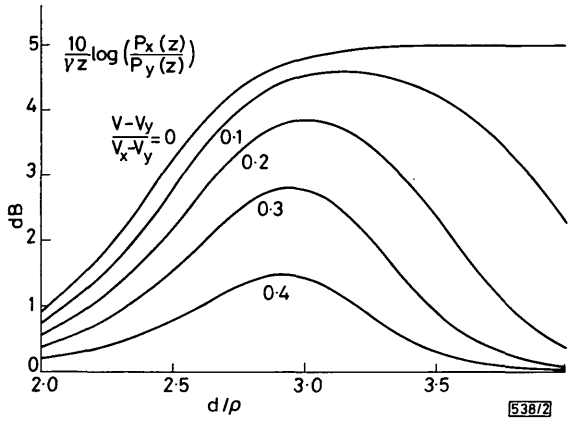

Fig. 2 *Normalised extinction ratio*

V_x and V_y are effective V values for x- and y-polarised modes of fibre 1, respectively, while V is the V value of fibre 2

Results: The normalised birefringence B is selected to be 5×10^{-4}; this can be achieved at present.[1-3] We take $V_y = 2$ and $V_x - V_y = 10^{-3}$, while $\Delta \simeq 5 \times 10^{-3}$. We vary the V value of the lossy fibre from V_y to $V_y + 0{\cdot}4(V_x - V_y)$ with five intermediate steps, and vary d/ρ from 2 to 4 on every step. The normalised extinction ratio is shown in Fig. 2. Since the polarisation mode we want to keep also suffers from some loss, we compare the extinction ratio with the loss of the wanted polarisation mode. Fig. 3 tells us the extinction ratio attainable for 1 dB loss of the wanted mode. If 0·1 dB loss of the wanted mode is acceptable, then the extinction ratio can be as high as 10^4 dB when $d/\rho = 4$. One important thing is that the extinction ratio is reasonably insensitive to the coupling condition, and Table 1 gives an example. Furthermore, we know from Reference 4 that

$$\frac{\delta\rho}{\rho} = \frac{1}{2\Delta} \frac{\delta\beta}{\beta} \frac{V^2}{U^2} \frac{K_1^2(W)}{K_0^2(W)} \quad (6)$$

where $\delta\rho/\rho$ is the perturbation of the fibre radius corresponding to $\delta\beta/\beta$, the perturbation of the propagation constant. Since $\Delta \ll 1$ for weakly guiding fibres, to adjust the radius of the lossy fibre is a practical way to match the coupling condition. For example, when $V = 2$ and $\Delta = 5 \times 10^{-3}$, then $\delta\rho/\rho \simeq 308\delta\beta/\beta$. If we want $\delta\beta/\beta = 0{\cdot}1B$, we have $\delta\rho/\rho = 15{\cdot}4\%$ when $B = 5 \times 10^{-4}$, and 15·4% is easy to obtain.

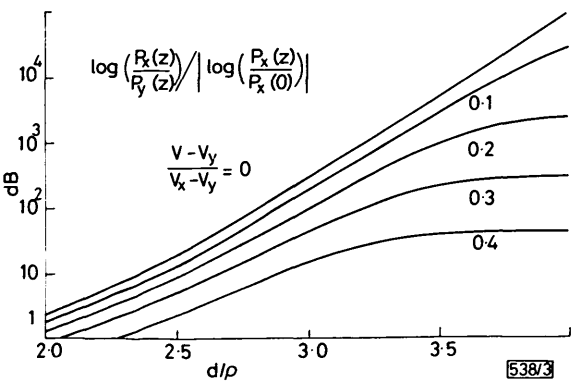

Fig. 3 *Comparison of extinction ratio and loss*

If α is the acceptable loss and η is the value found in the Figure, then an extinction ratio of $\alpha\eta$ can be obtained

Table 1 LOSS OF WANTED x-POLARISATION MODE AND EXTINCTION RATIO AFTER A FIXED DISTANCE WHEN COUPLING CONDITION DETERIORATES, $d/\rho = 4$

$\frac{V - V_y}{V_x - V_y}$	0	0·1	0·2	0·3	0·4
$10 \log\left(\frac{P_x(z)}{P_x(0)}\right)$	−0·06	−0·09	−0·15	−0·26	−0·48
$10 \log\left(\frac{P_x(z)}{P_y(z)}\right)$	500	234	35	7·4	1·9

Acknowledgment: The author wishes to thank Dr. A. Ankiewicz and Miss W. M. Henry for helpful discussions.

ZHENG XUE-HENG*

Optical Sciences Centre
Australian National University
Canberra, ACT 2600, Australia

* On leave from Shanghai University of Science & Technology, Shanghai, People's Republic of China

4th November 1986

References

1 RASHLEIGH, S. C., and MARRONE, M. J.: 'Polarisation-holding in a high-birefringence fibre', *Electron. Lett.*, 1982, **18**, pp. 326–327
2 BIRCH, R. D., PAYNE, D. N., and VARNHAM, M. P.: 'Fabrication of polarisation-maintaining fibres using gas-phase etching', *ibid.*, 1982, **18**, pp. 1036–1038
3 OKOSHI, T., OYAMADA, K., NISHIMURA, M., and YOKOTA, H.: 'Side-tunnel fibre: an approach to polarisation-maintaining optical waveguiding scheme', *ibid.*, 1982, **18**, pp. 824–826
4 SNYDER, A. W., and LOVE, J. D.: 'Optical waveguide theory' (Chapman and Hall, London, New York. 1983), pp. 570–572

RESOLUTION OF MOMENT EQUATIONS IN A NONLINEAR OPTICAL AMPLIFIER

Indexing terms: Optics, Nonlinear optics

In the letter a new method for the resolution of the moment equations in a nonlinear optical amplifier is exposed. Results for the four first moments for the saturated and unsaturated absorption cases are presented. These results are in good agreement with those obtained by other authors.

Introduction: The usual technique for the statistical description of the laser amplifier is based on the photon density matrix. Its diagonal elements give the differential equation which describes the temporary evolution of the conditioned probability density function $P_{n,m}(t)$ of having m photons in the considered mode and at an instant t when there were n photons at the amplifier input ($t = 0$). We will simply call this function $P_m(t)$. This differential equation can be expressed[1] as

$$\frac{dP_m(t)}{dt} = -\frac{(m+1)A}{1+(m+1)s} P_m(t) + \frac{mA}{1+ms} P_{m-1}(t) + \frac{(m+1)B}{1+(m+1)s} P_{m+1}(t) - \frac{mB}{1+ms} P_m(t) + (m+1)CP_{m+1}(t) - mCP_m(t) \quad (1)$$

where A and B are, respectively, the photon-stimulated emission and absorption coefficients, s is the saturation parameter and C is a coefficient representing other loss mechanisms, independent of the saturation phenomenon. It is a differential equation system which has been studied for some particular

cases by several authors.[2,3] In the absence of saturation ($s = 0$), the linear version is obtained, which corresponds to the equation given by Shimoda, Takahasi and Townes[4] for the quanta amplification.

Resolution method: The equation system describing the temporary evolution of the photon distribution moments is obtained from eqn. 1. For the rth-order moment we have

$$\frac{dm_r}{dt} = \sum_{j=1}^{r} \binom{r}{j-1} [\langle p_j(m)\rangle A + (-1)^{r+j-1}\langle q_j(m)\rangle B + (-1)^{r+j-1}\langle m^j\rangle C] \quad (2)$$

where

$$p_j(m) = \frac{(m+1)m^{j-1}}{1+(m+1)s} \quad (3a)$$

$$q_j(m) = \frac{m^j}{1+ms} \quad (3b)$$

and having defined the rth-order moment as $m_r = \langle m^r\rangle$.

For the different values of r, expr. 2 gives a coupled nonlinear equation system which is difficult to solve because of the dependence of each moment on the temporary evolution of all the others (in the linear case this dependence is just on the lower-order moments). Eqn. 1 has been studied by several authors without taking into account the loss mechanisms associated to the C coefficient. Particularly, Scully and Lamb[2] study the phenomenon of stimulated emission saturation but not that of the absorption. This would correspond to taking $C = 0$ and $q_j(m) = m^j$ in eqn. 2. Bendjaballah and Oliver[3] have proposed another model which also takes into account the absorption saturation. This is equivalent to simply taking $C = 0$ in eqn. 2.

From eqn. 2 for $C = 0$ we obtain

$$\frac{dm_r}{d\tau} = \sum_{j=1}^{r} \binom{r}{j-1} [\langle p_j(m)\rangle + (-1)^{r+j-1}\langle q_j(m)\rangle \beta] \quad (4)$$

where

$$\beta = B/A \quad (5a)$$

and

$$\tau = At \quad (5b)$$

Normalisations (eqns. 5*a* and *b*) have been done in order to enable an immediate result comparison with Reference 3. In this letter eqn. 4 is numerically solved instead of eqn. 1, to obtain the first-, second-, third- and fourth-order moments of the optical amplifier output photon distribution. To do so, functions $p_j(m)$ and $q_j(m)$ are developed in a Taylor series around the mean photon number $m_1(t)$. The software designed for the calculation of these developments allows calculations up to an arbitary order but less than or equal to the number of calculated moments. This is because the rth-order development statistical average value of the $p_j(m)$ and the $q_j(m)$ functions depends on the first r moment values $m_1(t), \ldots, m_r(t)$. The technique based on the development around the average value, combined with the step-by-step differential equation system numerical resolution obtained from eqn. 4, is very advantageous because, for a given precision required in the $m_r(t)$ calculation, it is not necessary to increase the development order as the average value increases with time. This would be the main problem if developments were done around the origin, because to maintain a constant error, development order should be progressively increased all through the amplification process. On the other hand, Hamming's predictor-corrector method has been chosen instead of the Runge-Kutta method, because of the need for two evaluations for the second member of eqn. 4 in each step, instead of the four evaluations per step needed by the Runge-Kutta algorithm for the same precision. Another advantage of Hamming's method is that in each step it gives an estimation of the truncating local error, which allows adequate calculation of the integration interval.

We will employ fourth-order developments to calculate the normalised moments, which we define as follows:

$$f_1(\tau) = \frac{m_1(\tau)}{m_1(0)} \quad (6a)$$

$$f_2(\tau) = m_1(0)g_2(\tau) \quad (6b)$$

and

$$g_i(\tau) = \frac{m_i(\tau) - m_1^i(\tau)}{m_1^i(\tau)} \quad (6c)$$

Results and conclusions: In Reference 3 Bendjaballah and Oliver present the normalised moments $f_1(\tau)$ and $f_2(\tau)$ for the linear, saturated absorption and unsaturated absorption cases. To compare our results with those of Reference 3 we have taken $\beta = 0{\cdot}9$, $s = 10^{-4}$ and a Poisson distribution at the amplifier input of average value $m_1(0) = 10^3$. In Fig. 1 the first-order normalised moment $f_1(\tau)$ is represented for the linear case (curve *a*) and nonlinear case with saturated absorption (curve *b*). Curve *c* in this Figure corresponds to the nonlinear case with unsaturated absorption. As might be expected, curve *c* takes lower values than curve *b* because the amplifier gain is lower than in the saturated absorption case. Obviously, both *b* and *c* curves are under the curve corresponding to the linear case (no saturation).

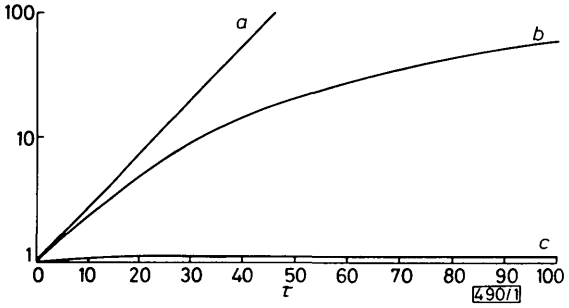

Fig. 1 *Plot of* $f_1(\tau)$

a Linear
b Saturated absorption
c Unsaturated absorption

Fig. 2 shows the second-order normalised moment $f_2(\tau)$ for the linear case (curve *a*), the saturated absorption case (curve *b*) and the unsaturated absorption case (curve *c*). The values obtained for this set of magnitudes are almost exactly those published by Bendjaballah and Oliver. In their work they comment in a clear and concise way on their meaning.[3,5] Third- and fourth-order normalised moments $g_3(\tau)$ and $g_4(\tau)$ are also represented in this letter (Fig. 3). Curves *a* and *b* correspond to the third-order moment for the saturated and unsaturated absorption cases, respectively. In a similar way, curves *c* and *d* correspond to the fourth-order moment for the same cases.

All the graphs have been calculated for 50 intermediate points of the dimensionless variable τ. The calculation of more points does not give an appreciable improvement in the values of the different normalised moments. In particular, the choice

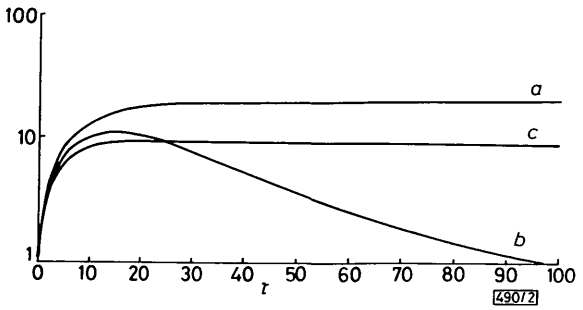

Fig. 2 *Plot of* $f_2(\tau)$

a Linear
b Saturated absorption
c Unsaturated absorption

of 100 points produces changes in the fourth decimal place. The relative error in the plotted curves is of about 10^{-4} in the worst case. Fourth-order developments have been employed for the calculation. The computing time for the calculation of

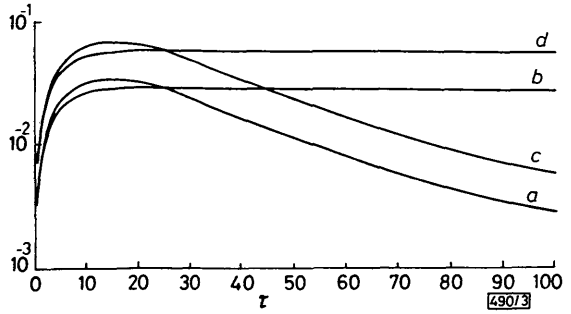

Fig. 3

Plot of $g_3(\tau)$ and $g_4(\tau)$ [*a*, *b* and *c*, *d*, respectively] for saturated and unsaturated absorption [*a*, *c* and *b*, *d*, respectively]

the first four normalised moments was approximately 8 min working with the standard Fortran compiler in a Perkin-Elmer 3200 computer. To obtain just the first two normalised moments, second-order developments can be employed, which give a 10^{-2} precision in 30 s computation time. Taking into account the obtained results and computation time, we can conclude that the resolution method exposed in this work is effective. It must be emphasised that increasing the development order above 4 does not produce remarkable improvements in the precision of the results.

S. RUIZ-MORENO
G. JUNYENT
J. R. USANDIZAGA
A. CALZADA

Department of Communications
ETSIT Barcelona
c/Jorge Girona Salgado s/n
08034 Barcelona, Spain

21st October 1986

References

1 YAMAMOTO, Y.: 'A.M. quantum noise in semiconductor lasers-Part I: Theoretical analysis', *IEEE J. Quantum Electron.*, 1983, **QE-19**, pp. 34–46
2 SCULLY, M. O., and LAMB, W. E. JR.: 'Quantum theory of an optical maser. I. General theory', *Phys. Rev.*, 1967, **159**, pp. 208–226
3 BENDJABALLAH, C., and OLIVER, G.: 'Comparison of statistical properties of two models for saturated laser light amplifier', *Phys. Rev. A*, 1980, **22**, pp. 2726–2731
4 SHIMODA, K., TAKAHASI, H., and TOWNES, C. H.: 'Fluctuations in amplification of quanta with application to maser amplifiers', *J. Phys. Soc. Jpn.*, 1957, **12**, pp. 686–700
5 OLIVER, G., and BENDJABALLAH, C.: 'Statistical properties of coherent radiation in a nonlinear optical amplifier', *Phys. Rev. A*, 1980, **22**, pp. 630–634

MOLYBDENUM GERMANIDE OHMIC CONTACT TO *n*-GaAs

Indexing term: Semiconductor devices and materials

GeMo refractory ohmic contacts for *n*-type GaAs with a specific contact resistivity as low as $10^{-6}\Omega cm^2$ have been obtained on $10^{18} cm^{-3}$ epitaxial layers. This low resistivity was obtained by contact annealing under As overpressure. Contacts using As-doped Ge layers and annealed without As overpressure have also been realised; in this case the obtained resistivity was $5 \times 10^{-6}\Omega cm^2$. The ohmic contact formation resulted from the creation of an n^+ layer by Ge overdoping and the formation of a molybedenum germanide stable phase.

Introduction: High-reliability refractory ohmic contacts are required to process devices such as self-aligned heterojunction bipolar transistors for which a stable contact is necessary to afford the annealing treatment subsequent to the *p*-type implantation.

The classical AuGeNi alloyed ohmic contact has been extensively studied for *n*-type GaAs,[1] but this contact exhibits a severe degradation above 450°C and is not suitable for the control of small dimensions. Molybdenum germanide has already been investigated[2] because it should provide low specific contact resistivity and good thermal stability on GaAs. Moreover, it could be selectively etched on GaAs, thus allowing ood dimensional control.

In this letter we report the successful realisation of GeMo/GaAs ohmic contacts with Ge and Mo thin layers (150 Å thick). Auger electron spectroscopy (AES) combined with transmission electron microscopy (TEM) analysis were carried out to study the species diffusion and the contacting metallurgy formation. We will discuss the influence of the As overpressure on the contact formation.

Experiment: The metals were deposited on *n*-type GaAs layers ($n = 10^{18} cm^{-3}$) grown by molecular-beam epitaxy. Pure or As-doped Ge was deposited first using electron-beam evaporation with a background pressure of 10^{-7} torr and a deposition rate of 10 Å/s, while Mo was sputtered in an RF plasma with a deposition rate of 2 Å/s. The thickness of each layer was 150 Å. A tungsten protective layer (1000 Å) was then deposited by RF sputtering.

Annealing was performed in a halogen lamp furnance under a forming gas (Ar, 10% H_2) in the case of As-doped Ge, and in a conventionnal thermal furnance with an As overpressure in the case of pure Ge.

The specific contact resistivity was determined by the transmission-line method (TLM).[3]

Results: The influence of As overpressure on the ohmic contact formation has been investigated. In a first experiment, contacts using pure Ge and annealed without As overpressure have been tested. It was found that, whatever the annealing conditions, the electrical behaviour was nonohmic. In the case

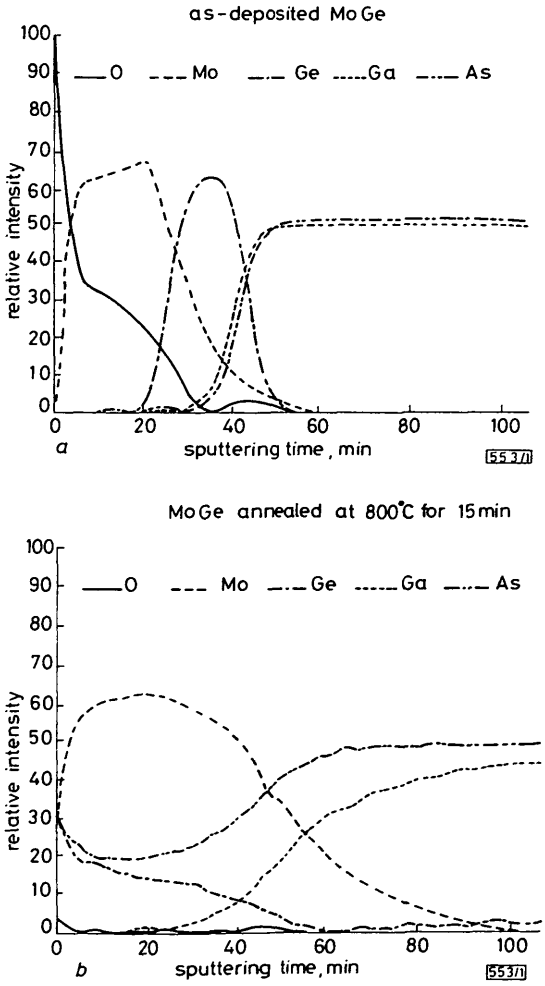

Fig. 1 *AES profiles of 150 Å Mo/150 Å Ge/GaAs (a) as-deposited and (b) annealed at 800°C, 15 min, under As overpressure*